Available online at www.sciencedirect.com

ScienceDirect

Procedia Structural Integrity 28 (2020) 132–138

Structural Integrity Procedia

www.elsevier.com/locate/procedia

1st Virtual European Conference on Fracture

Mechanical behavior of Nd:YAG laser welded aluminum alloys

Girolamo Costanza[a)*], Maria Elisa Tata[b)]

[a]*Industrial Engineering Department, University of Rome Tor Vergata, Via del Politecnico, 1- 00133, Rome, Italy*
[b]*Computer Science and Civil Engineering Department, University of Rome Tor Vergata, Via del Politecnico, 1- 00133, Rome, Italy*

Abstract

Al alloys, conceived for automotive and aeronautic applications thanks to the high strength/density ratio, exhibit weldability issues common to all light alloys. In particular loss of toughness and soundness of welded joints consequent upon welding operations, possible cracking in the weld metal and metallurgical modifications induced in the heat affected zone. In this paper the weldability of AA2139, AA6110 and AA6156 with the same filler of AA4047 was investigated by comparing features of welds carried out by Nd:Yag laser process. Some samples have been welded of different Al alloys. Welded joints were submitted to optical and SEM metallographic examinations with EDS. Microanalysis measurements were performed to evaluate locally chemical composition and to investigate the nature of the precipitates. Mechanical properties were evaluated through tensile test (T-pull and Hoop stress) and fatigue test (T-pull and Hoop stress). One of the main results is the goodness of this kind of welding between the different alloys for mechanical properties and metallographic features. In particular the configuration AA6156-AA2139-AA4047 is typical for resistance structure in aircraft applications, consisting in extruded AA2139 stringer, responsible to absorbing structural loads and AA6156 skin with high corrosion and crack propagation resistance.

Keywords: Al alloys, Laser welding, Nd:YAG, mechanical properties, t-pull, hoop stress.

1. Introduction

Aluminum alloys, due to the high mechanical resistance/specific density ratio, are very attractive for the needs of the automotive and aeronautic industry as evidenced by Immarigeon et al. (1995), Wagner (2005) and Warner (2006).

* Corresponding author. Tel.: +39-06-72597185; fax: +39-06-2021351.
E-mail address: costanza@ing.uniroma2.it

10.1016/j.prostr.2020.10.017

In the car body design, for example, the extensive adoption of lightweight materials can reduce the vehicle's fuel consumption and decrease pollutant emissions. More in general, as highlighted by Ringer et al. (2000) and Kumar et al. (1996), Al Alloys of the series 2000 (Al-Cu-Mg), containing Cu as the main alloy element, exhibit optimal mechanical properties after aging thermal treatment and are suitable for service temperatures up to about 150° C. The 6000 series (Al-Mg-Si) are also precipitation – hardening alloys, like the 2000 series, and the morphology and distribution of the precipitates dictate mechanical properties and environmental response of the alloy. With the addition of elements like Mg and Li it is possible to reduce the specific density on one side and to improve performance for structural applications on the other side as evidenced in their works by Calogero et al. (2014), Doglione (2005), Heinz et al. (2000), Kazanijan et al. (1997) and Starke et al. (2000).

Weldability of Al alloys is a very important issue, as illustrated by Irving (1994), Rading et al. (1998), Costanza et al. (2016), Costanza et al. (2018). Limitations are usually determined by macroscopic features (irregularities in the bead, cracks, porosity etc.) and by metallurgical defects in the MZ (dendritic structure, segregations, dilution, etc.), in HAZ (overaging, recrystallization structure etc.) and stress (macro and micro stress following thermal welding cycles) as discussed in Heinz et al. (2000), Janaki Ram et al. (2000). The welding reliability of Al alloys is lower than that of other industrial metals due to its higher reflectivity, higher thermal conductivity and lower viscosity. Therefore dealing with Nd-YAG laser welding process its reflectivity, lower than that of the CO_2 laser, allows to get better welding and less defects as demonstrated by Kuo et al. (2006). The welding properties can be changed with filler materials having composition to follow the satisfactory structures after dilution with the base metal. In the HAZ, mechanical properties could be restored with post welding heat treatments. An assessment of weldability can be made by comparing the results of mechanical tests (tensile strength, toughness, fatigue etc.) on welded joints with base metal; Heinz et al. (2000); Bonaccorsi et al. (2012).

In this study the attention is focused on the use of Nd-YAG laser technologies for welding of aluminium alloys. It is well known that 6xxx series aluminum alloys are weldable but the alloys of 2xxx series show more defects. Some samples have been prepared of different weldings; at first with two different families of Al alloys (2XXX and 6XXX) separately and finally with two families joined together. The tested welds have three different combination of materials: 1) AA6156-AA6110-AA4047; 2) AA2139-AA2139-AA4047. 3) AA6156-AA2139-AA4047. Mechanical behavior has been investigated with tensile and fatigue tests. Metallographic characterization has been performed by means of stereo, optical and scanning electron microscope. One of the main results is the goodness of this kind of welding between the different alloys for the mechanical properties and the metallographic characteristics.

Nomenclature

HAZ	heat affected zone
MZ	molten zone

2. Materials and methods

The examined materials are the following aluminium alloys: AA2139, AA4047, AA6110, AA6156. The first one (AA2139) is an Al-Cu-Mg-Ag based alloy with high corrosion resistance. It was T3 heat treated as received and after the welding process it has undergone T8 heat treatment with an artificial ageing. The AA6110 and AA6156 alloys are traditional Al-Mg-Si alloys. Main properties of this alloys are corrosion resistance, mechanical resistance and good weldability. Differently from AA2139, AA6110 and AA6156 alloy are more corrosion resistant but shows lower mechanical properties. For this reason AA6XXX alloys are usually employed only where the corrosion aspect is the main characteristic. Despite belonging to the same family, AA6156 has been laminated while the AA6110 alloy has been extruded. This specification is important because they can be used respectively for the skin or stringer in the fuselage of an aircraft. For both of them a high damage tolerance (DT) is required, i.e. more resistance to the crack propagation. These alloys are T4 heat treated as received while after the welding process a T6 heat treatment has been necessary in order to achieve the optimal mechanical properties in the MZ. The AA4047 is a traditional alloy in this field characterized by a good weldability and therefore it has been chosen as filler. The chemical composition (wt.%)

of these alloys are shown in table 1 and the mechanical properties of as received alloys and in test conditions in table 2.

Table 1. Chemical composition (wt. %) of AA2139, AA4047, AA6110 and AA6156 alloys.

Alloy	Si	Fe	Cu	Mn	Mg	Zr	Ti	Ag	Cr	Zn
AA2139	0.05	0.06	4.95	0.29	0.43	0.014	0.005	0.33	-	-
AA4047	12	0.8	0.3	0.15	0.1	-	-	-	-	-
AA6110	0.6-1.3	0-0.5	0.3-1.1	0.2-1	0.6-1.2	0-0.01	0-0.1	-	0-0.25	0.1-0.7
AA 6156	0.6-1.0	0-0.5	0.6-1.1	0.2-0.8	0.8-1.2	-	0-0.01	-	0-0.2	0-0.25

Table 2. Mechanical properties of AA2139, AA6110, AA6156 at 25 °C.

Alloy and thermal treatment	Yield strength (MPa)	Tensile strength (MPa)	Elongation after fracture (%)
AA2139 As received (T3)	345	425	16
AA2139 Test condition (T8)	430	475	12
AA6110 As received (T4)	220	320	16
AA6110 Test condition (T6)	360	380	10
AA6156 As received (T4)	210	265	18
AA6156 Test condition (T6)	360	380	8

A sketch of the T-joint of tested samples between stringer and skin is reported in Fig. 1

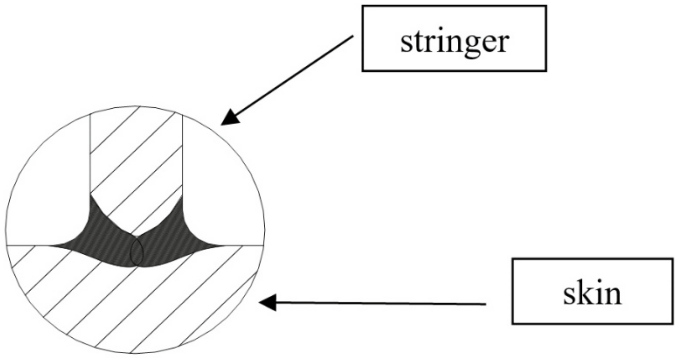

Fig. 1. Sketch of the T-joint between stringer and skin.

Table 3. Welding configurations.

Welding configuration	skin	stringer	filler
1st	AA6156	AA6110	AA4047
2nd	AA2139	AA2139	AA4047
3th	AA6156	AA2139	AA4047

In order to reproduce the stress in the real operating conditions the test configurations have been T-pull and Hoop-stress, as shown in Fig. 2. In the pull test the possible separation of the skin from the stringer has been simulated as well as the radial stress the fuselage is subjected to. In the second configuration (hoop) the stress is applied in line with the skin in order to reproduce the circumferential stress.

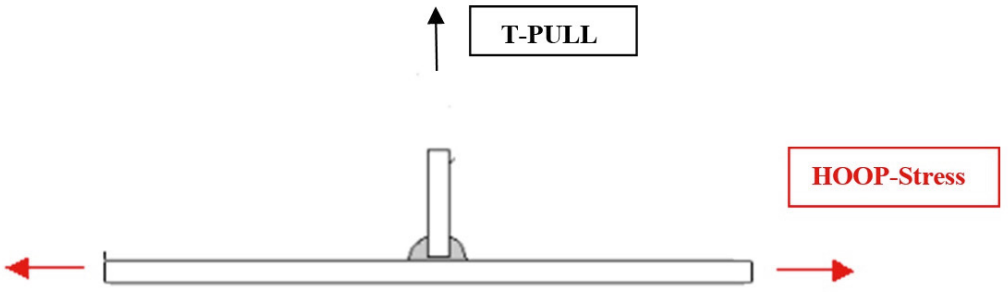

Fig. 2. Sketch of the T-PULL specimen and Hoop specimen.

For welding two Nd-YAG lasers have been used, based on Neodymium-doped (Nd^{+++}) yttrium aluminium garnet crystal as active medium. The following technical specifications have been adopted: max power 4kW, spot diameter 0.6 mm, focal distance 200 mm, collimation length 200 mm, max welding speed 100 mm/min, protective gas mixture Ar and He. MTS 810 machine has been employed for tensile and fatigue tests (minimum/maximum stress ratio R = 0.1, frequency 15 Hz). Metallographic characterization has been performed by means of stereo, optical and scanning electron microscope (SEM) with EDS microanalysis. For microstructural characterisation samples have been polished and subjected to chemical etchant with Keller solution (1.0 ml HF, 1.5 ml HCl, 2.5 ml HNO_3, 95 ml H_2O).

3. RESULTS

Stereo microscope observations allow to identify the geometry of the molten zone, in particular: the symmetry of the MZ, the penetration deep inside the skin and possible defects in the weld. In the first configuration of joint (AA6156-AA6110-AA4047) the penetration of the MZ inside the skin is about 45% of the thickness of the skin while the lower side of the MZ presents a little asymmetry between the right side and the left one (Fig. 3 a). In the second configuration of joint (AA2139-AA2139-AA4047) a little asymmetry of the molten zone is present too in the MZ and the penetration of the MZ inside the skin is about 30% of the skin thickness. No other macroscopic defects have been evidenced from this analysis.

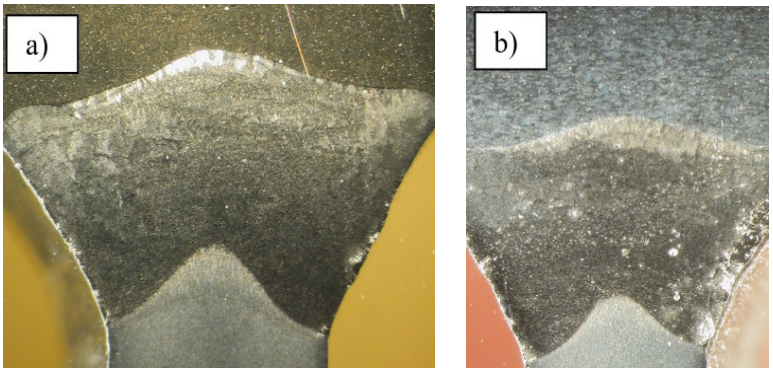

Fig. 3. a) Stereo microscope observations on joint configuration (AA6156-AA6110-AA4047); b) configuration 2 (AA2139-AA2139-AA4047).

After mechanical polishing and keller chemical etching some sections of the joints have been analyzed. Optical microscope observations are reported in Fig. 4.

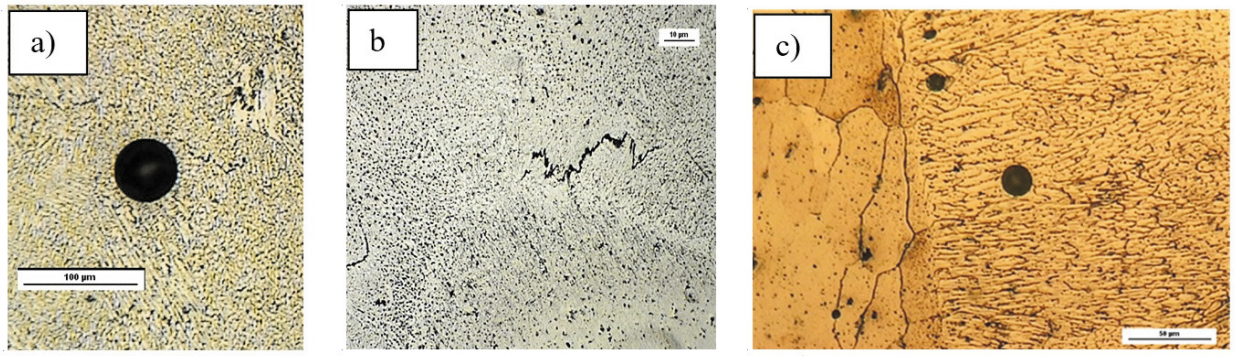

Fig. 4. a) Porosity in MZ; b) crack in MZ AA6156-AA6110-AA4047; c) porosity in MZ AA2139-AA2139-AA4047.

In the first joint (AA6156-AA6110-AA4047), Fig. 4 b) shows a crack in the upper side of the MZ, near the stringer. In the second joint, (AA2139-AA2139-AA4047) Fig. 4 c), the symmetry of MZ is acceptable though small porosities have been evidenced. For what concerns the HAZ in the first joint (AA6156-AA6110-AA4047) the HAZ is about 80-90 µm (Fig. 5 a). EDS microanalysis on some particular star-shaped structures, detected between MZ and the stringer component, reveals zones richer in Mg, Si and Cu than the 6110 alloy. In the second joint (AA2139-AA2139-AA4047) the HAZ is about 115-120 µm (Fig. 5 b), only small porosities have been found and negligible amounts of star-shaped structures.

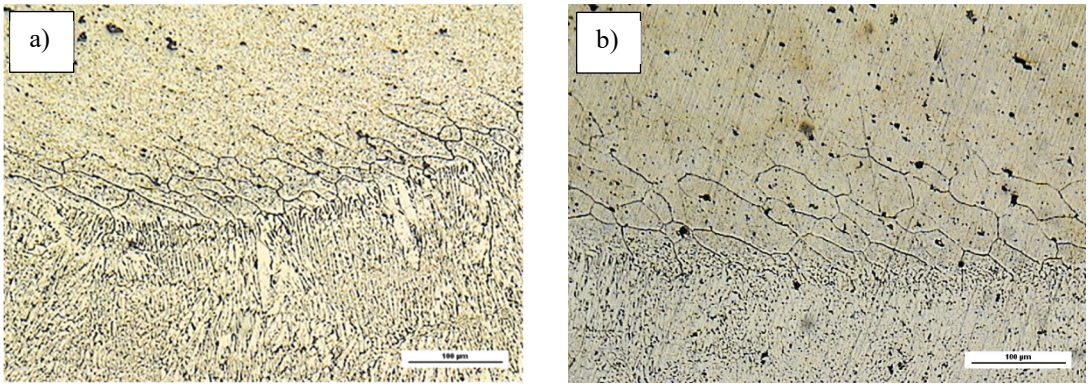

Fig. 5. a) HAZ AA6156-AA6110-AA4047; b) HAZ AA2139-AA2139-AA4047.

Results of mechanical testing are reported on Tab. 4 and 5 for hoop stress and T-pull stress respectively: ultimate strength and elongation for AA6156-AA6110-AA4047, AA2139-AA2139-AA4047 and AA6156-AA2139-AA4047.

Table 4. Static Hoop test results for AA6156-AA6110-AA4047, AA2139-AA2139-AA4047 and AA6156-AA2139-AA4047.

Test sample	Ultimate Strength (MPa)	Elongation (%)
AA6156-AA6110-AA4047	380	4.4
AA2139-AA2139-AA4047	466	8.9
AA6156-AA2139-AA4047	337	7.9

Table 5. Static T-pull test results for AA6156-AA6110-AA4047, AA2139-AA2139-AA4047 and AA6156-AA2139-AA4047.

Test sample	Ultimate Strength (MPa)
AA6156-AA6110-AA4047	370
AA2139-AA2139-AA4047	452
AA6156-AA2139-AA4047	390

According to the results of the tensile tests (ultimate strength) it has been possible to identify the stress value to be applied in the fatigue tests in the T-pull and Hoop stress configurations. Fatigue test results in terms of Wohler curves in the three weld configurations are reported in Fig. 6. In the diagrams σ_{max} is the maximum stress applied and N the number of cycles to failure.

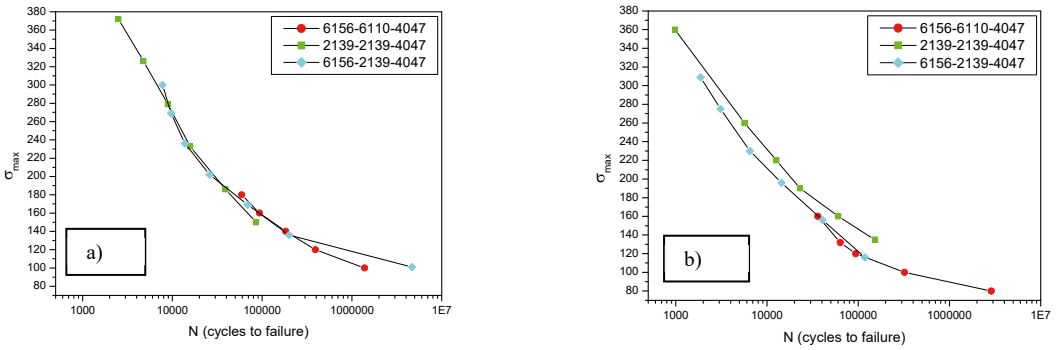

Fig. 6. a) Hoop stress fatigue test results; b) T-pull stress fatigue test results.

In the hoop stress fatigue test the AA6156-AA2139-AA4047 showed the best fatigue behaviour, in terms of number of cycles to fracture under the same applied stress. From the analysis of the fracture surface it has been evidenced that cracks start in the area where both skin and stringer material are present. Cracks propagation, however, occurs exclusively in the skin material. Hence the following conclusions: alloy AA6156 shows a better fatigue behaviour, i.e shows the higher resistance to crack propagation. For the T-pull test the optimal performance has been found with AA2139-AA2139-AA4047. This result is in line with the static test ones. At last, the AA6156-AA2139-AA4047 behaves slightly better than AA6156-AA6110-AA4047 in the hoop test and in the middle between the three configurations studied, thus resulting in the T-pull an excellent coupling.

4. DISCUSSION AND CONCLUSIONS

Metallographic examinations show that AA6156-AA6110-AA4047 weld is quite inhomogeneous, affected by various defects such as microcracks, porosities and intermetallic phases. On the other hand, the AA2139-AA2139-AA4047 weld appears quite homogeneous and free of relevant defects. For both static hoop stress and T-pull tests the higher ultimate strength values were obtained in AA2139-AA2139-AA4047 weld. Also fatigue tests confirmed that the higher mechanical behaviour for hoop stress tests and T-pull test was reached by AA2139-AA2139-AA4047 weld. Considering the mechanical test results and the metallographic examinations, the best weld is AA2139-AA2139-AA4047. Its mechanical properties are similar to those of the base metal.

Since the design criterion for the skin component is “damage tolerance”, it is required for the alloys to show resistance to dynamic loads, crack propagation and corrosion resistance. The adoption of weldings instead of rivets for joining alloys means that the so-called “break crack”, or the hole of the fasteners, are missed so the materials itself will have to make up this lack. Regarding the corrosive agents, the skin is one of the parts most exposed to the

atmospheric phenomena therefore it is very important the corrosion resistance of the structure. In the case of the stringer, the design criterion is tensile behaviour that is very important in terms of mechanical properties. The selection of AA2139 alloy as stringer is motivated by the fact this alloy, containing Cu and Ag, shows higher mechanical behaviour. As regards the choice of material for the skin, the optimal selection is AA6156 alloy due to the good corrosion resistance and better crack propagation resistance as evidenced from the fatigue test results. In conclusion among the three combinations analyzed, the AA6156-AA2139-AA4047 alloy shows suitable properties for the considered application. The last one has been tested too and has shown a more homogeneous microstructure with less defects, reduced weld area was (60 μm) in comparison with 80-90 μm of AA6156-AA6110-AA4047 and 115 μm of AA2139-AA2139-AA4047. Furthermore the lower part of the weld bead is asymmetrical and the depth of penetration in the skin is about 28% of the thickness. Finally the third configuration has a resistant structure consisting in extruded AA2139 stringer, responsible to absorbing structural loads, and a AA6156 skin with high corrosion resistance and crack propagation resistance.

References

Bonaccorsi, L., Costanza, G., Missori, S., Sili, A., Tata, M.E., 2012. Mechanical and metallurgical characterization of 8090 Al-Li alloy welded joints. Metallurgist 56 (1-2), 75-84.

Calogero, V., Costanza, G., Missori, S., Sili, A., Tata, M.E., 2014. A weldability study of Al-Cu-Li 2198 alloy. Metallurgist 57 (11-12), 1134-1141.

Costanza, G., Tata, M.E., Cioccari, D., 2018. Explosion welding: process evolution and parameters optimization. Materials Science Forum 941, 1558-1563.

Costanza, G., Crupi, V., Guglielmino, E., Sili, A., Tata, M.E. 2016. Metallurgical characterization of an explosion welded aluminum/steel joint. Metallurgia Italiana 108 (11), 17-22.

Doglione, R., 2005. Le leghe alluminio litio. Metallurgia Italiana 2, 39-50.

Immarigeon, J.P., Holt, R.T., Koul, A.K., Zhao, L., Wallace, W., Beddoes, J.C., 1995. Lightweight materials for aircraft applications. Materials Characterization 35 (1), 41-67.

Heinz, A., Haszler, A., Keidel, C., Moldenhauer, S., Benedictus, R., Miller, W.S., 2000. Recent development in aluminium alloys for aerospace applications. Materials Science and Engineering A 280 (1), 102-107.

Irving, B., 1994. Welding the four most popular aluminum alloys. Welding journal 73 (2), 51-55.

Janaki Ram, G.D., Mitra, T.K., Raju, M.K., Sundaresan, S., 2000. Use of inoculants to refine weld solidification structure and improve weldability in type 2090 Al-Li alloy. Materials Science and Engineering A 276 (1-2), 48-57.

Kazanijan, S.M., Wang, N., Starke, E.A. 1997. Creep behavior and microstructural stability of Al-Cu-Mg-Ag and Al-Cu-Li-Mg-Ag alloys. Materials Science and Engineering A 234-236, 571-574.

Kumar, K.S., Brown, S.A., Pickens, J.R., 1996. Microstructural evolution during aging of an Al-Cu-Li-Ag-Mg-Zr alloy. Acta Materialia 44 (5), 1899-1915.

Kuo. T.Y., Lin, H.C., 2006. Effect of pulse level of Nd-YAG laser on tensile properties and formability of laser weldments in automotive aluminum alloys. Materials Science and Engineering A 416 (1-2), 281-289.

Rading, G.O., Shamsuzzoha, M., Berry, J.T., 1998. A model for HAS hardness profile in Al-Li-X alloys: application to the Al-Li-Cu Alloy 2095. Welding journal 77 (9), 382-387.

Ringer, S.P., Hono, K., 2000. Microstructural evolution and age hardening in aluminium alloys: atom probe field-ion microscopy and transmission electron microscopy studies. Materials characterization 44 (1-2), 101-131.

Starke, E.A., Sanders, T.H., Cassada, W.A., 2000. Metallurgical design of alloys for aerospace structures. Materials Science Forum 331-337, 5-16.

Wagner, V., 2005. Evoluzione delle leghe d'alluminio per aeronautica dopo le due guerre mondiali. Metallurgia Italiana, 6, 9-21.

Warner, T., 2006. Recently developed aluminum solutions for aerospace applications. Materials Science Forum 519-521, 1271-1278.